COMPULSATOR DESIGN FOR ELECTROMAGNETIC
RAILGUN SYSTEM

By

Bryan Bennett

Senior Project

Electrical Engineering Department

Cal Poly State University,
San Luis Obispo

June, 2012

ABSTRACT

This project designed, fabricated, and partially tested a compensated pulsed alternator (compulsator) to power an electromagnetic rail gun (EMRG) in a multidisciplinary team. The EMRG team includes two master's AERO students, two senior EE students, and three senior ME students. Design of the compulsator began with research through conference and research papers. This design was changed throughout the project as system analysis and component testing exposed unforeseen system limitations. While original specifications were not met, all fabricated components but one, the stator, were completed using Cal Poly's facilities and the project's limited available budget. Experimental verification of calculations and system modeling were not obtained because the compulsator was fully assembled at the time of this writing, but the necessary measurements and testing procedures have been outlined.

TABLE OF CONTENTS

LIST OF FIGURES

LIST OF TABLES

ACKNOWLEDGEMENTS

INTRODUCTION

This system was designed with the goal of increasing the energy density of an electromagnetic railgun's (EMRG) power supply, thus reducing its footprint. The EMRG was designed to offer a low cost alternative to orbital debris testing on satellites. The current technology for testing, light gas guns, require large facilities to operate and are very expensive to employ. Jeff Maniglia, a Master's Aerospace Engineering student, has designed the EMRG to accelerate particles to geosynchronous speed. His current discharge system is capacitive and drives the EMRG to half of his lowest desired speed. To increase this speed the capacitor bank must greatly increase in size and would become difficult to test. The final bank that could reach the upper limit of orbital speeds would not be mobile.

The goal of this senior project is to explore EMRG power supplies with higher energy densities than the current capacitive system by designing and fabricating a compensated pulsed alternator (compulsator). Design began with research into conference papers, theses, and any other literature on compulsators that could be found online. Once a basic topology had been decided upon, general electric motor equations were used to find approximate requirements for the machine while the system was being modeled to test the validity of these approximations. The required magnetic field was calculated using Faraday's Law of Induction. The mechanical engineer's working on the project determined that 5000 rpm was the maximum safe rotation speed of a rotor sized to fit the fabrication facilities available at Cal Poly. The field strength and rpm requirements were used to determine the number of turns on the rotor and stator.

Once the basic motor calculations were completed, research into the pulse forming compensation aspects of compulsators began. Passive compensation methods were chosen for their easy of construction. Commutators were explored along with winding schemes with the goal of minimizing resistance and inductance in the system. System safety was of prime importance during this advance stage of design. Safety measures included large safety factors and worst case assumptions in calculations, internal components used to control the large magnetic shift that occurs during discharge and prevent damages to pulse forming components, and large alterations to the anchoring and housing of the EMRG test bed to ensure containment of a worst case structural failure during full spin.

Fabrication and testing of various components forced changes to the design towards the end of the project. The errors discovered were caused by miss reading website data sheets in ignorance, reaching the limits of materials and available fabrication facilities, and by the ever present limitations of time and budget. The changes to the design allowed the construction of the compulsator to continue but would not allow for system specifications to be met. More than twice the funding that was available for the year of work on the compulsator will be available for the next team project with the EMRG, so it is the hope of the EMRG team that this compulsator will be the prototype that gives the next team the necessary information and materials to meet an even more demanding set of system specifications.

BACKGROUND

Compulsators offer greater energy densities and can be operated with less infrastructure and cost than the current orbital impact testing facilities. There are two classes of compulsator: iron cores, in which the rotor is constructed of a ferrous material, and air cores, in which the rotor is constructed of a non-ferrous material. Iron core rotors have large amounts of mass thus spin at relatively low speeds, 5,000 - 10,000 rpm. The rotor in an air core compulsator is much lighter in comparison and operates at higher speeds, 10,000 – 20,000 rpm. Air core machines are significantly more expensive and difficult to machine than iron core machines. While iron cores present less of a challenge to produce their ferrous cores can reach saturation in the strong fields required to generate the compulsator's large output. Saturation of the core will limit the maximum possible output of an iron core machine but will not be an issue with the current EMRG power supply requirements.

Capacitive systems require pulse forming components, such as resistors and diodes, that increase the footprint. While these components do not seem large as they are used in so many circuits, it is important to remember that tens of thousands of amps are being discharged through these networks and the components within them must be sized accordingly. Compulsators include all of the pulse forming within the machine in the form of compensation and commutation. Compensation is passive or active and in most cases reduces the mutual inductance seen between field and armature windings. Passive methods include thin sheeting wrapped around the rotor windings to reduce the maximum inductance seen during discharge. Commutation rectifies the output internally. Active methods include compensation windings which create fields that reduce the inductance of the windings they are in series with.

The downside to compulsator systems is that they require exact tolerances in design and fabrication. During design, milliohms and microhenrys are all that can be allowed in the system to achieve reasonable system outputs. Fabrication tolerances are all in the thousandths of an inch. The balancing and centering of shafting must be maintained to reducing vibrations in the machine because there will be significant physical stresses during discharge.

Compulsators are more difficult to fabricate than capacitive systems but could still replace them if they exceed the capacitive systems capabilities in two key areas: the size of the power supply and EMRG together and the cost of testing with that set up.

Size aspect:

The compulsator must have a small footprint to maximize the mobility of the EMRG test bed. To increase the utility of the EMRG for testing small satellites in many different situations it must be able to test in and out of a vacuum chamber and to change locations as necessary of any client. The current EMRG is one meter long and with accompanying discharge system occupies a single 3'x5' table top. A compulsator could theoretically be built that would reach the required power for the upper limit of geosynchronous speeds and safely housed on a concrete slab twice the size of the EMRG table. The corresponding capacitive system would fill an 8' x 8'x5' room.

The current facilities that can reach the maximum speeds are very large and expensive. In Figure 1 below, a composite picture of NASA's light gas gun is shown. It is a composite picture because the gun is too long to fit into a single image while retaining detail.

Figure 1: NASA's light gas gun [3]
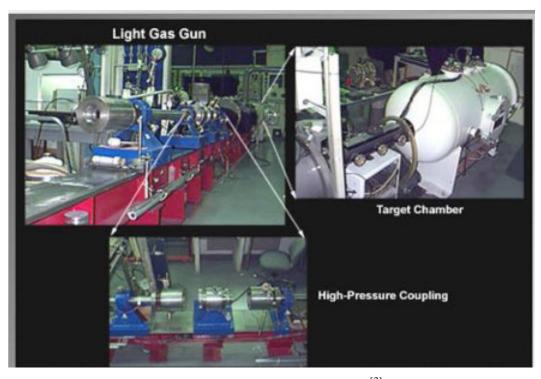
Other forms of acceleration, such as shaped charges, can reach these speeds but degrade the projectile significantly and cannot offer repeatable cross sections and masses from their tests. Both of these systems are limited by the speed of the expanding gasses used as propellants, thus the energy storage and barrel of the gun take up considerable space while limiting the maximum

velocity. Compulsator driven EMRGs are theoretically only limited by the current carrying capabilities of their components, giving those systems a greater maximum velocity.

Cost aspect:

Operating light gas gun test beds can cost thousands of dollars a minute. Multiple tests can take hours to complete. Whatever testing environment that has been built along with the gun will be fixed at its end and would be costly to change. A compulsator driven system would be able to operate with less infrastructure and overhead. Changing the test environment would be easier with a mobile system. For instance, firing at a target in and out of a vacuum would only be a matter of moving the compulsator to and from the vacuum chamber. Also, the Cal Poly EMRG can be operated with a minimum of man power. The majority of staff working on the testing will be students and would require less compensation for their time than industry professionals with years of experience. The funds from testing fees would be put back into funding for further pulsed power based senior projects or master theses. The initial investment into the compulsator is high, but the system can be designed for cost efficient refits of key components that will extend the life time of the machine.

REQUIREMENTS

System Requirements:

The goal of this system is to supply an EMRG with a 450 V, 100 KA square pulse. To meet this requirement with the current EMRG load, the resistance of the entire compulsator must be on the order of 1×10^{-3} Ω. This energy will be built up in the compulsator by spinning it up with a prime mover and discharged in such a way as to allow the compulsator to begin the spin up process again after reaching full stop.

Pulse Requirements:

Pulse ripple that does not cause the output voltage to dip below the ignitron conduction minimum, 150 V, is acceptable. The pulse width must be greater than 1.5 ms and less than 5 ms to obtain the maximum acceleration from the projectile as it travels down the barrel without wasting any of the energy in the pulse. This is done by ensuring that the pulse has finished before the projectile leaves the barrel.

Foot Print Requirements:

The compulsator must be no larger than 4'x4' including all supporting materials such as the prime mover, testing equipment, and switching circuitry. All of these will fit on a concrete base. The concrete base must be massive enough to absorb any vibrations generated by the system while still being able to be moved by a fork lift. The size of the base will be dictated by the safety requirements for discharge which include the physical barrier that must be built around the compulsator to contain structural failures and the size of the approved testing area.

Lifespan Requirements:

The compulsator must be able to fire multiple times without the refit of internal components. Neutral plane shifts, specifically the arching across the commutator that these cause, are the most common cause of damages and must be paid special attention. Because each firing will begin from full stop and the projectiles will be press fit into the EMRG's breach, rapid firing of the compulsator driven system will not be possible. 25-50 full speed firings without refitting is the goal. The machine should run for at least 20 hours on refits of the commutator and its brushes before a thorough rebuild is required.

Total System Design

This project consists of two main components: the stator and the rotor. The stator houses the magnetic poles and the interpoles. The rotor is lap wound with an aluminum conduction shield around the windings and connects to the commutator. See Figure 2 for a circuit diagram of the system.
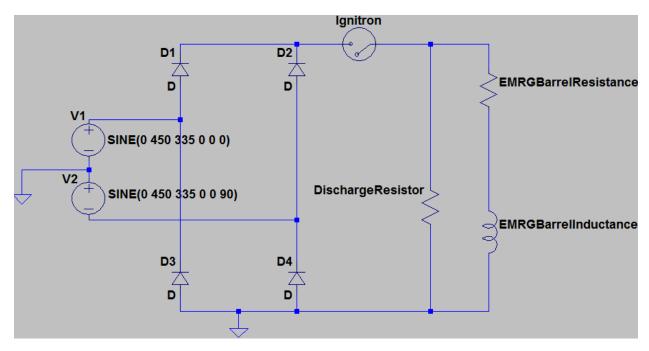

Figure 2: Circuit diagram of the complusator system

Figures 3 and 4 on the next page show a cross section of the stator and a cross section of the entire assembled machine respectively. These images were prepared by the mechanical engineers as part of their system modeling. In Figure 4, 1 points to a pole magnet rail, 2 points to an interpole, 3 points to the magnets that have been secured to the magnet rail with epoxy, 4 points to the flange interpoles which secure the two halves of the stator together, and 5 points to the half inch diameter bolts that will secure the magnet rails and interpoles to the stator. The stator housing has the highest tolerance requirements so it was the only component that was sent to professional facility to be fabricated.
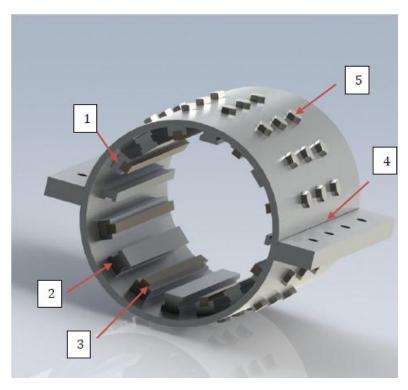
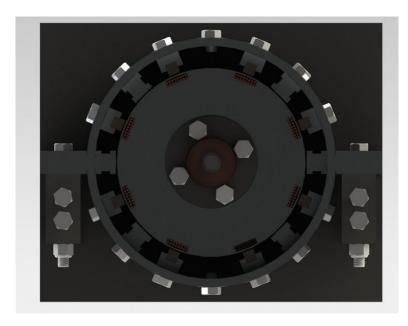Figure 3: Assembled stator alone with components annotated

Figure 4: Assembled compulsator cross section

The following equation gives the flux density required to induce 450 V in the machine given a number of windings on the rotor. [18]

$$B = \frac{V_{rms}}{\sqrt{2} * \omega_r * A * N}$$

V_{rms} is the voltage induced in one phase on the rotor and is required to be 450 V_{rms}. ω_r is the angular velocity of the rotor. A is the cross-sectional area of the rotor. N is the number of turns in one of the phase on the rotor. The maximum number of windings was determined by the mechanical engineering students to be twenty turns with 14 AWG wire. The required flux density was calculated to be 1.25 tesla.

The following equation gives an approximation of the required current to produce B in a set of field windings housed on the stator.[18] It is an approximation because the stator windings are not perfectly modeled by a current in a solenoid with a cylindrical core but is close enough for the initial exploration of the system and its costs.

$$i = \frac{Bl_c}{\mu N}$$

B was calculated above. l_c is the mean path length of the core used for the windings and is 0.2335 meters. μ is the permeability of aluminum. N is the number of turns in the field windings. Table 1 shows the current required to produce a 1.25 T field in various numbers of stator winding turns.

Stator winding turns	I [A]
400	580.6539531
380	611.2146875
360	645.171059
340	683.1222978
320	725.8174414
300	774.2052708
280	829.5056473
260	893.313774
240	967.7565885
220	1055.73446
200	1161.307906
180	1290.342118
160	1451.634883
140	1659.011295
120	1935.513177
100	2322.615812
80	2903.269766
60	3871.026354
40	5806.539531
20	11613.07906

Table 1: Current required to produce a 1.25 T field given a number of turns

Magnetic Poles:

The data in Table 1 shows that a high current is necessary to produce the flux density required to meet specifications. Even with conservative estimation on wattage requirements, a power supply that could meet these requirements ranged from $400 to $1800 dollars, even with a combination of used and donated supplies. Adding to this cost would be the special magnet wire designed to minimize resistance and inductance called Litz wire that the windings would be constructed of. Finally, there was a tradeoff between the number of windings that could be wound on the stator and the amount of heating the system could handle. The heating is generated by larger currents running through copper windings. Design difficulties and a cost that was outside of the limit placed on individual components during initial designs required the selection of another method of generating the required field. A 10000 W power supply was donated to the project at a later date but the lab that is used for testing the EMRG in not equipped with the three phase inputs the supply required.

Permanent magnets were selected instead because it was believed that they were more cost effective than a power supply. The use of permanent magnets will not allow for the use of compensation windings for increased flux compression during discharge because there are no field windings for them to be wound in series with. In theory the compensation windings could be made to work with the magnets but this was outside our knowledge of permanent magnets and could do more harm than good if not done correctly. Safety was a key concern when designing this machine and the difficulty of finding any documentation that derived equations for the use of compensation windings with permanent magnets suggested that undergrads should not attempt to build something that could not be proven in theory or simulations.

Initially, custom fabricated magnetic rails that would span the length of the rotor were explored, but the cost of these magnets was greater than the windings and power supply combined. More research found half inch cube neodymium boron iron magnets at rare-earth-magnets.com. These were listed as 1.25-1.28 T magnets with an operating temperature limit of 80 C^o. [1]

The magnets must be mounted on an aluminum rail so that they span the entire ten inch length of the rotor. The magnets were epoxied into the rails, alternating which pole was exposed on top. Figure 6 is an image taken from the mechanical engineer's FEA analysis on the magnetic rails.
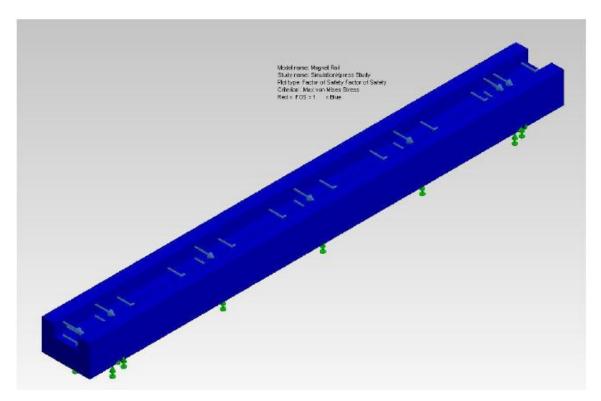
Figure 5: FEA simulation of aluminum mounting rail for permanent magnets

Material Choice:

Aluminum was chosen as material for the stator, interpoles, and magnet rails because its permeability is close to that of air and because it aids in construction and placement of the magnetic rails by being non-ferrous. A ferrous material would cause the magnets to attract every part of the stator, hampering fabrication. Aluminum was also cost effective, structurally strong, and easily machined. Initially modern composites were explored but were found to be too difficult and time consuming to manufacture. The mechanical engineering students performed the analysis for all of the materials aspects of the machine.

Interpoles:

During discharge, an effect called armature reactance occurs and it can cause damage to the commutator brushes and segments. When the ignitrons trigger, completing the circuit between the EMRG and compulsator, the energy in the rotor is discharged through the armature windings. This current running through the armature windings will produce a magnetic field around the rotor. Without this field, the commutator is at zero potential when connecting

segments on the commutator, giving the desired rectified output with arching between the segments and the brushes. This plane where the adjacent commutator segments are at zero potential is called the neutral plane. If this plane shifts, adjacent segments on the commutator will have a potential difference and arcing will occur on the commutator, causing damage and potentially pocking the surface of the commutator or brushes to the point of destroying their functionality. This effect is called neutral plane shift.

Neutral plane shift can be counteracted by placing an axillary set of poles in between the magnet rails. These poles, called interpoles, will be tied to the output of the commutator and will only receive power during discharge. The interpoles are wound to produce the same pole that would come next in the rotation. The armature reaction causes a large force on the rotor in opposition to the direction of rotation during spin up, shifting the neutral plane in the same direction. It is important to connect the interpoles in parallel with the output because the discharge phase of the compulsator is so transient. To design a control system that could supply the correct amount of current within the 3 ms pulse width would be extremely difficult. When in parallel with the output, the interpoles can be given a divided output that will scale with the entire output pulse and corresponding armature reactance. As the output increases the armature reaction forces the neutral plane to shift in the opposite direction to the spin up rotation and the interpoles shift it back by a corresponding amount, negating the plane shift.

The interpoles must have the same polarity as the pole that comes next in the rotation of the machine. See Figure 7 below for the order of the poles.
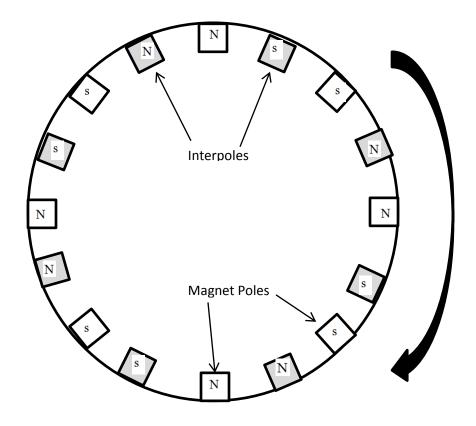
Figure 6: Pole orientation given direction of rotation, interpoles in grey

The following equations give the required density of the interpoles and the required number of interpole turns given the number of turns on the rotor and the desired interpole current. [19]

$$\text{Armature} \frac{\textbf{AT}}{\textbf{pole}} = \frac{\textbf{I}_{armature} * \textbf{Z}}{2 * \textbf{a} * \textbf{P}}$$

$$\text{Flux density} = \textbf{B} = \textbf{F} * \frac{\textbf{u}}{\textbf{l}_{armature}}$$

$$\text{Interpole turns} = \textbf{N}_{interpole} = \frac{\textbf{B} * \textbf{l}_{interpole}}{\textbf{u} * \textbf{i}_{\max\_interpole}}$$

The number of turns on the rotor was five and the desired interpole current was 4 A. Table 2 and Table 3 below calculate the required field strength of the interpoles and the number of turns required to produce that field.

Stator Turns	AT/pole	Required density [T]
100	125000	0.27856557
95	118750	0.264637292
90	112500	0.250709013
85	106250	0.236780735
80	100000	0.222852456
75	93750	0.208924178
70	87500	0.194995899
65	81250	0.181067621
60	75000	0.167139342
55	68750	0.153211064
50	62500	0.139282785
45	56250	0.125354507
40	50000	0.111426228
35	43750	0.09749795
30	37500	0.083569671
25	31250	0.069641393
20	25000	0.055713114
15	18750	0.041784836
10	12500	0.027856557
5	6250	0.013928279
1	1250	0.002785656

Table 2: Required interpole field strength

Interpole Imax [A]	Interpole Turns
1600	0.069272034
1500	0.07389017
1400	0.079168039
1300	0.085257888
1200	0.092362712
1100	0.100759322
1000	0.110835254
900	0.123150283
800	0.138544068
500	0.221670509
300	0.369450848
100	1.108352545
80	1.385440681
70	1.583360778
60	1.847254241
50	2.21670509
40	2.770881362
30	3.694508483
20	5.541762724
10	11.08352545
4	27.70881362

Table 3: Number of interpole turns

Armature windings:

The armature or output windings are wound around the stator. There are many different windings schemes available so a list of key features was made. The scheme must minimize system resistance, must maximize output current while maintain the minimum conduction voltage of the ignitrons, must not create large connections on the commutator to assure mechanically and electrically sound connections and that the brush pads can fit within the stator housing, and finally must be able to be wound by hand. Many winding schemes either use preformed windings and special rotor slots or use automatic winding machines and schemes optimized for them. Duplex lap windings were chosen because they offer parallel paths that reduce the overall resistance of the machine. This winding scheme produces low voltages and high output currents.

The coil or pole pitch determines the where the connections from each coil will fall on the commutator. The following equation calculates the pole pitch. [4]

$$pole\ pitch = y = \frac{S}{P}$$

S is the number of slots on the rotor and P is the number of poles. If the first connection from a coil is placed on segment A of the commutator the then the second connection must be placed on segment A + y. A diagram of one set of slots with windings and the layout of the conductors within the slot can be found below in Figure 8.
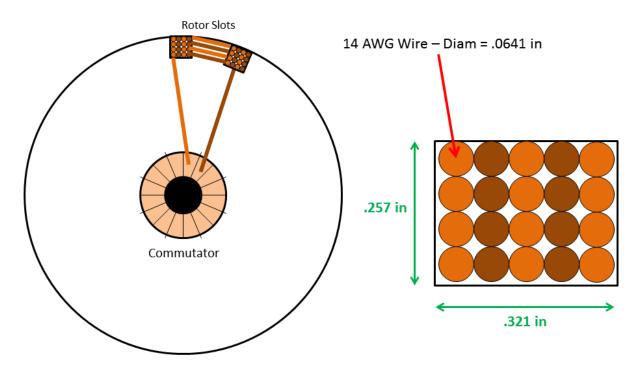

Figure 7: Proposed winding scheme

The resistance of the windings was calculated as a worst case first without any parallel paths, just the resistance found in the total length of copper used for the windings. The equation for the total length of the armature windings can be found below.

$$l_{total} = l_{phase} * 2 = 2(l_{single\ turn} * N + l_{commutator})$$

The total length is equal to two times the length of one turn, $l_{single\ turn}$, times the number of turns, N, plus the length of wire needed to make the commutator connections. Our total length of

wire was 33.5 feet. The resistance of 14 AWG copper wire is 0.00118 Ohms/ft so our total resistance without parallel paths was 0.03953 Ohms.

Commutator:

   A commutator was donated that has sixteen segments up to eight pads. It did not have any kind of connectors attached, just bare copper. Initially different clips and hooks attachments such as in Figure 9 below were explored as modifications to the donated commutator, but the mechanical engineers were not confident that the small hooks or clips could be mechanically secured in a way that could tolerate the large stresses produced during full spin and discharge. The reason for this is because 14 AWG wire would require very large hooks to be attached. Braising directly to the commutator segments will be the joining method.

Figure 8: Commutator with hooks for connections [2]

SYSTEM MODELING

Ordinary Differential Equations:

Ordinary differential equations, ODEs, attempt to model system performance with respect to time with simple differential equations that do not involve partial derivatives. By examining theses and research papers, Collin MacGregor was able to construct a set of instantaneous equations. These equations were verified in electrical engineering books and deemed valid by this author, though not all aspects of the final ODE is understood. I was unable to verify equations dealing with compulsator compensation methods or total system inductances. The equations resulting from the compulsator topology only were unable to be verified simply because there are no other sources of material other than literature online. The system inductance was not verified because of the steep learning curve of Finite Element Method (FEM) magnetic simulations. Attempts were made to model the system in Ansoft's Maxwell, but these models could not be cross checked with the ODEs because the simulations were never made to coverage to a solution. Some values can be generated but they are not being listed due to uncertainty in their validity.

Once the instantaneous equations were verified, Collin produced a state space that propagates the system performance. A large Matlab program was created that takes EMRG system variables such as resistance, inductance, angular velocity, the position of the particle in the EMRG, and the compulsators peak discharge current as arguments and produces graphs of the system output and expected performance. The stored mechanical energy with respect to time and $\frac{dI}{dt}$ are both approximate equations because governing equations for the exact topology of the compulsator, permanent magnets and passive compensation, were not found. These equations were modeled after several other topologies that contained similar aspects to the teams chosen topology and are believed to be a good approximation for worst case scenarios and safety factors, but more complete and detail analysis of the topology should be completed before design of the next compulsator begins. The accurate and complete system modeling of the EMRG and compulsator system is the subject of Collin's Master's thesis. These equations are listed here because some input was given in their creation and because they played a critical role in the analysis and first construction phases when changes to the design were forced. Equations will be listed first followed by definitions of their variables.

<u>Instantaneous voltage equation:</u>

$$V(t) = V_0 * \sin(\omega_e t)$$

$$V_0 = N_p * N_{cp} * l_r * B * v_{tip}$$

$$v_{tip} = \frac{(RPM) * \pi * D_r}{60}$$

$$\omega_e = \frac{\omega * N_{pairs}}{2 * \pi}$$

$$V(t) = \left[N_p * N_{cp} * l_r * B * \left(\frac{(RPM) * \pi * D_r}{60} \right) \right] * \sin\left[\left(\frac{\omega * N_{pairs}}{2 * \pi} \right) * t \right]$$

V_0 = rotational emf (V), ω_e = electrical frequency (s^{-1}), and t = time (s). N_p = number of poles in rotor, N_{cp} = number of conductors per pole on rotor, l_r = length of rotor (m), B = field strength density (T), and v_{tip} = rotor tip speed (m/s). RPM = rotations per minute of rotor and D_r = diameter of rotor (m). ω = mechanical angular velocity (rad/s) and N_{pairs} = number of pole pairs (the number of north, south pole face combinations).

<u>Instantaneous inductance equation:</u>

$$L(t) = L_{min} * \rho * sin(\omega_e * t - \delta)$$

$$\rho = \frac{1}{2}\left(\frac{L_{max}}{L_{min}} - 1 \right)$$

$$L(t) = L_{min} * \left[\frac{1}{2}\left(\frac{L_{max}}{L_{min}} - 1 \right) \right] * sin\left[\left(\frac{\omega * N_{pairs}}{2 * \pi} \right) * t - \delta \right]$$

$$i(t) = \frac{\Phi(t)}{L(t)}$$

L_{min} = minimum inductance of compulsator (H), ρ = compulsator inductance modulus, and δ = electrical phase angle (rad). L_{max} = maximum inductance of compulsator (H). $\frac{L_{max}}{L_{min}}$ = the flux compression ratio of the system. i(t) = instantaneous current, $\Phi(t)$ = flux linkage of the compulsator with respect to time, and $L(t)$ = inductance of the compulsator with respect to time.

ODEs:

$$\frac{d\omega}{dt} = \frac{-\sqrt{\frac{2VI}{J_r}}\,dt}{dt}$$

$$E = \frac{1}{2}J_r\omega^2$$

$$\frac{dx}{dt} = \sqrt{2\frac{d^2x}{dt}x}$$

$$\frac{d^2x}{dt} = \frac{L'I^2}{2m}$$

$$\frac{dI}{dt} = \frac{V - I(R_c + R_o + R'x) + I\left(\omega_e L_{min}\rho \sin(\omega_e + \delta) - L'v_p\right)}{L_{min}(1+\rho) + L + L'x + L_o}$$

$$v_p = \frac{dx}{dt}$$

J_r = rotor inertia (kg-m^2), V = voltage of compulsator system (V), dt = time step, and I = total compulsator discharge current (A). x = particle position along railgun (m) and is zero for initial condition. L' = inductance gradient of rails (H/m) and m = mass of projectile (kg). R_c = compulsator's internal resistance (Ω), R_o = resistance of connecting bus bar (Ω), L_o = inductance of connecting bus bar (H), R' = resistance of the railgun (Ω), and v_p = particle velocity inside the railgun (ms^{-1}).

From the $\frac{dI}{dt}$ equation on page 20 it can be seen that the resistance and inductance play critical roles in system performance. Maximizing performance requires minimal resistance and a flux compression ratio of one. The inductance is a critical variable because compulsators operate in transient regime of power generation during acceleration and deceleration. In a general sense a lower inductance and resistance lowers the time constant of the system, allowing it to discharge its energy faster. Flux compression ratios larger than one can increase the overall efficiency of the machine but also produce larger physical stresses during discharge. Large ratios could not have been used due to safety concerns and because the peak inductance must still be on the order of microhenrys meaning that the minimum inductance must be even lower. Achieving that level of inductance is very difficult in iron core machines. To ensure safety, a flux compression ratio of one was desired. This means that the inductance of the machine should change as little as possible during discharge.

Figure 9 below and Figure 10 on the next page are system output and performance graphs respectively. They have been calculated using optimal values in which the compulsator's inductance and resistance have been matched to the load. The target resistance was 1 mΩ and the target inductance was 10 µH. Figure 11 on the next page and Figure 12 on page 23 are the same graphs with the resistance increased to 10 mΩ.
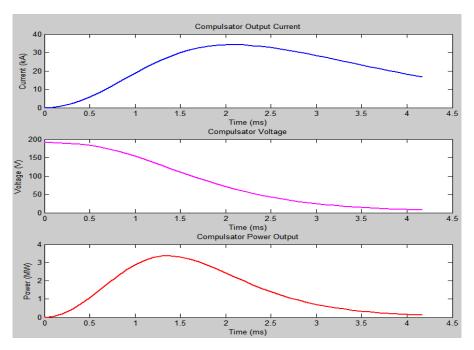
Figure 9: Compulsator output during discharge, optimal resistance
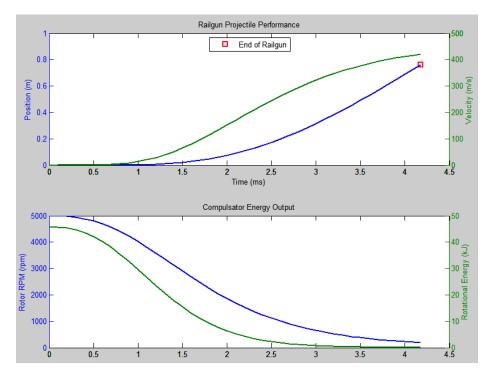
Figure 10: Railgun performance and compulsator total energy output, optimal resistance
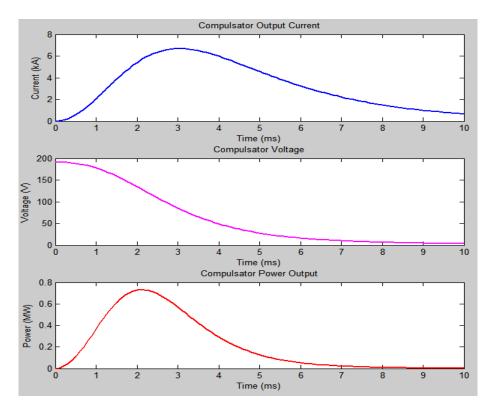
Figure 11: Compulsator output during discharge, increased resistance
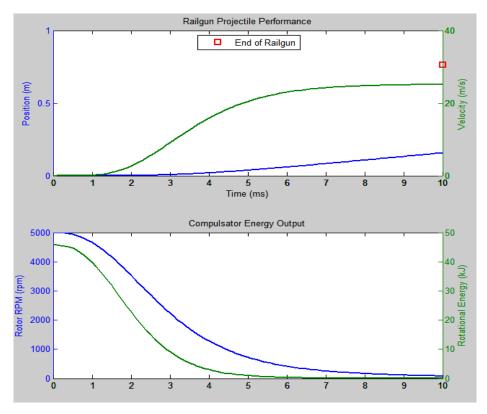
Figure 12: Railgun performance and compulsator total energy output, increased resistance

Figures 9-12 demonstrate the effect of increased resistance in the system. Milliohms are enough to degrade they system performance from ballistic velocities of 400 m/s to just 20 m/s or roughly 45 miles per hour. This means that every component from the armature windings to commutator brushes and even the short connections between the ignitrons and the rails of the EMRG must have its resistance carefully measured and minimized. Besides the armature windings, all resistances are considered to be in the worst case series connection.

Magnetic simulations were attempted with Maxwell and FEMM but both programs proved difficult to use. The difficultly came in understanding what types of boundary conditions needed to be used between the complex boundaries of air, aluminum, and permanent magnets found in many places on the stator. Even when modeling one quadrant of the stator and rotor without rotation, the net list of nodes was in the tens of thousands. With net lists of this size and topologies with the complexity of the compulsator, solution attempts can take tens of iterations and many hours to complete. Without enough iterations and proper system set up the programs were unable to converge to a solution and what data was extracted could not be verified. Appendix C contains the image of the first model created in FEMM.

ANALYSIS AND TESTING

Magnets:

The characterization of the magnets began with the marking the north and south faces on each magnet. To do this the magnets were allowed to connect together. Since the connecting faces must be a north/south pair, the top and bottom of the pair must be North and South respectively. The field strength of each magnet was measured using a PASCO PASPort magnetic field sensor. This was done because a 300 gauss difference in the poles could cause translational forces in the machine. The equation below gives the force on the armature winding.

$$F = i(l \times B)$$
$$F = i * l * B * \sin(\theta)$$

i is the current in the wire, l is the length of the wire, B is the magnetic flux density, and Ө is the angle between the wire and the flux density vector. The worst case scenario of completely opposite windings with the maximum tolerance difference during discharge will give a difference of 42 KN. The mechanical engineers said that translational forces must be minimized to ensure safe operation. By mixing the strengths of the magnets on each rail and placing magnets with fields closest to 1.25 T on the end of the rails, the tolerance in fields between each rail is minimized.

Because the magnets were believed to have a field strength of over a tesla, the hall effect sensor would not be able to take surface measurements of the field because the limit of the sensor was 1000 gauss [16]. My first attempt to find a way to measure the magnets involved creating my own sensor. The sensor was simply a hall effect element and an amplifier. Unfortunately hall effect elements with the lowest resolution, 0.1 mV/gauss, could only measure up 2500 gauss [4]. Normally the element is given a supply voltage in the middle of its operation range. A north pole produces a positive increase in voltage and the difference between that and the supply is proportional to the field strength. A south pole will produce a voltage drop in the hall effect element. Trying to use the hall effect with the lowest possible supply voltage and then only measuring north faces would ensure that voltages were kept within limits while being able to measure the maximum range allowable by the component. When this was attempted it was

found to be too difficult to keep from having any drop in voltage occur from the south pole. The hall effect element was destroyed with a small percentage drop below its operational minimum.

By measuring the field strength from a distance the PASPort sensor could be used to find a relative strength. The equation below can be solved for the distance from the magnet given the field strength. The equation was solved using MatLab.

$$B_X(X) = \frac{B_R}{\pi}\left[\tan^{-1}\frac{A*B}{(2X)\sqrt{4X^2 + A^2 + B^2}} - \tan^{-1}\frac{A*B}{2(L+X)\sqrt{4(L+X)^2 + A^2 + B^2}}\right]$$
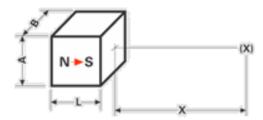
Figure 13: Drawing of magnetic flux density at distance X [5]

B_r is the remnant flux density and the rest of the variables are defined in Figure 13. During this initial testing B_R was an unknown variable. After researching the term it was found that this corresponded to the magnet's constitute materials ability to maintain a flux density after the magnetizing field is removed. [17] After reviewing the information given on the website where the magnets were purchased it was found that what was thought to be the surface field, B, was actually the remnant flux density. Most of the magnet distributors found online reported the remnant value as it is significantly larger than the surface field for neodymium boron iron magnets. This meant that the magnets were approximately one third of the strength originally designed for. Further research showed that the maximum surface field strength that can be obtained with neodymium boron iron magnets was 7000 gauss with most magnets falling in the 3500-5500 gauss range. The magnets that had been ordered were 4950-5050 gauss. Permanent magnets were not a viable choice for the project specifications but how the magnetic values were commonly reported online was not known during the design process. Because of the cost of the magnets and the time frame in which the error was discovered, an alternative to the magnets could not be obtained. The problem was partially addressed with changes to the winding scheme as detailed in the analysis of the windings in the next section.

Once this mistake was accounted for it was realized that the calculation of the distance X away from the magnet did not change with this new knowledge. A field strength of 500 gauss and a 0.5 inches for all other dimensions were entered into the equation. 500 gauss was selected to place the sensor in the center of its range of operation to ensure that the tolerance of the magnets would not place the sensor near the limits of operation. Then the equation was solved for X using MatLab to give a value of 0.458 inches. The sensor was firmly secured to the test bench and then the magnets were placed in a non-ferrous jig to ensure that they were set the same distance away from the sensor with each measurement. Table 4 on page 27 shows the measured fields for the first half of the 200 magnets ordered. The entire dataset was not included because very little variation is found in the magnets and the first grouping of measurements clearly shows this.

The rails used to house the magnets securely to the stator were ten inches long with a 0.125 inch deep channel along its length. These required twenty magnets each to complete one pole face of the four pole machine. The extra magnets were purchased to allow for some losses during construction. A steel jig was fashioned with a similar channel that has blocked ends to fix the magnets in place.

A ferrous material was used for the jig because when attempting to place the magnets in a row it was found that they difficult to force flush against each other. The downward force of the magnets against the steel helps to counter act this. It was found that the magnets repulsed so strongly because cube magnets are not magnetized completely axially. The equation for calculating the repulsive force between two cylindrical bar magnets is given below.

$$F = \left[\frac{B_0^2 A^2 (L^2 + R^2)}{\pi \mu_0 L^2} \right] \left[\frac{1}{x^2} + \frac{1}{(x + 2L)^2} - \frac{2}{(x + L)^2} \right]$$

Where B_0 is the surface flux density in tesla, A is the area of each pole in meters^2, L is the total length of each magnet in meters, R is the radius in meters and was approximated as 0.3175 centimeters, and x is the distance between the two magnets in meters. This equations was used as an approximation of the force between two cube magnets due to the difficultly of solving the equation in its cube form (see equation on page 27 for an example of the difficulty in dealing with cube magnets). The repulsive force of the magnets was 125 N or 28.1 pounds force.

Magnet	Measured B [gauss]	Magnet	Measured B [gauss]	Magnet	Measured B [gauss]	Magnet	Measured B [gauss]
1	535	26	562	51	531	76	553
2	521	27	530	52	532	77	530
3	532	28	531	53	542	78	536
4	530	29	532	54	550	79	564
5	545	30	532	55	530	80	532
6	531	31	530	56	536	81	531
7	535	32	550	57	539	82	539
8	573	33	541	58	530	83	536
9	535	34	537	59	531	84	530
10	530	35	530	60	540	85	530
11	542	36	531	61	530	86	531
12	550	37	525	62	521	87	545
13	538	38	540	63	529	88	547
14	561	39	541	64	526	89	530
15	530	40	552	65	530	90	563
16	531	41	533	66	531	91	530
17	535	42	530	67	519	92	543
18	530	43	538	68	530	93	535
19	529	44	530	69	537	94	530
20	545	45	532	70	540	95	531
21	530	46	530	71	542	96	540
22	532	47	543	72	537	97	552
23	530	48	534	73	535	98	532
24	530	49	556	74	532	99	527
25	531	50	569	75	549	100	522

Table 4: Measured magnetic flux density at 0.458 inches for 100 magnets

A graph produced on kjmagnetics.com was included that also uses a cylindrical approximation for repulsive force in Figure 14 and was included to show that calculations done by hand match other literature online. The values given by this equation can only be used as a relative approximation because it was based on Gilbert's model of repulsing dipoles which is only accurate at separation distances greater than the length of the magnet. [7] The repulsive force calculation was used to ensure that the magnets would not repulse with such strength as to cause the epoxy to fail when the magnets were under the combined stress of the machine at full spin up. The tensile strength of the epoxy used is roughly 10000 psi [8] so as long as the magnets do not repulse with a force greater than ten percent of this the rail will still be with the safety factors required by the mechanical engineering students.
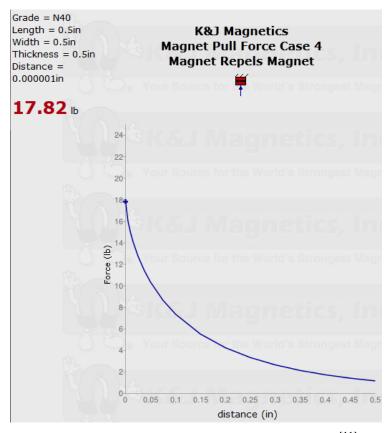
Figure 14: Force vs. Distance for N40 magnets [11]

The large steel jig was also used because the magnets were strong enough to attract the face that another magnet was resting on from over half an inch away. These magnets were powerful and dangerous to work with. Proper care must always be taken when handling magnets

28

like this such as removing all electronics and ferrous materials from the work space and having a large area of space to spread the magnets out when working with them. This ensures that the magnets do not snap together from a large distance. Fingers can be pinched between the colliding magnets potentially causing damage up to and including broken bones or chipping sharp pieces from the brittle magnets.

<u>Windings:</u>

Because the magnets were nearly one third of the strength that was designed for, the number of windings on the rotor needed to be increased to salvage some of the projected output. Due to eddy currents and distance from the magnetic field, windings do not continue to linearly increase the output of the machine even though the governing equations suggest that this could happen. The eddy currents occur most prominently at the corners of the rotor slot and the effects of these currents are amplified the deeper the slot is. Other slot designs could have reduced this effect but would have increased machining difficultly and increase the time spent on rotor fabrication. The number of slots on the rotor was also increased to sixteen to create two phases with the same number of windings.

The depths of the channels in the rotor were increased by sixty percent to allow for twelve turns of 10 AWG wire. The decrease in wire gauge was made to decrease the resistance per kilometer. The winding scheme was also changed to duplex, the most allowed by the number of phases in the machine. In this scheme there is one segment between each end of one set of windings for one phase. The next ends of the next phase are placed on the next pads, one of which is in between the ends of the previous phase. This provides two separate paths for current and, assuming all the paths have the same resistance, divides the winding resistance by two.

Because system resistance must be minimized, a tradeoff between the number of turns in a slot and the number of parallel paths must be met. While more turns do produce greater output power, greater system resistance more quickly degrades performance. Because this it was decided to braze two ends of windings to each commutator pad, doubling the number of parallel paths to four but reducing the number of turns per phase by half. More ends could not be attached to the same commutator segment because of the area limitation of the segment and of the rotor slots. Figure 16 depicts the new winding scheme. Note that the different colored

windings in the slot correspond to the two parallel paths introduced by the single connection on the commutator segment.
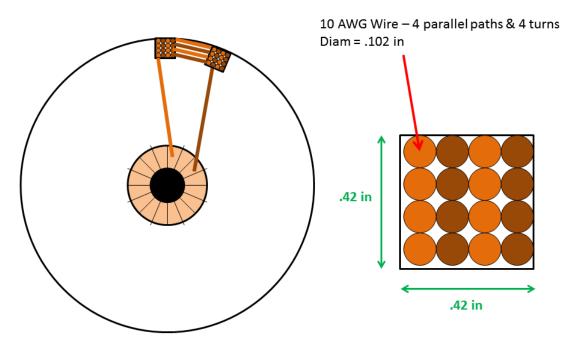
Figure 15: New winding scheme with separation of three segments

Resistance Measurements:

      Every part of the compulsator needed to have its resistance accurately measured. The difficulty in measuring the resistance of component such as the commutator brushes arises from the resistance in the testing leads of digital multi-meters (DMM). DMMs supply a constant known current to the component being tested through the leads and then use a voltmeter to measure the voltage across the component. The voltage and current measurements are then used to calculate the resistance with ohms law. The voltage measurement will include the drops from the resistances in the leads. Even with short leads, grabber and banana probes will have resistances on the order of 0.05-0.1 mΩ, which is 1-10 percent of the measurements made. To counteract this a 4-wire (Kelvin) meter was used. This meter has four leads that are electrically separated, two of which have low resistance and connect to an ammeter. The other two leads connect to a voltage through high resistance leads to minimize current through the voltmeter. This limits the drops across the leads and gives an accurate measurement. See Figure 17 below for a diagram of the meter and connections. Note that the halves of the clips at the end of the

leads are electrically separated and only complete a circuit when the ends touch around the wire that the measurement is being take from.
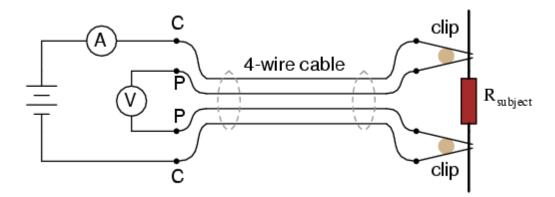
Figure 16: Kelvin meter circuit diagram

Using the 4-wire meter it was found that the commutator brushes originally purchased had a resistance of 5 mΩ. This resistance was close to the resistance desired for the entire system and had to be reduced. The original brushes were constructed of carbon only which offers an excellent contact surface with the commutator leading to near perfect commutation at the expense of resistance and system efficiency. Since the pulse requirements are very loose with the actual shape of the pulse, brushes that degrades uniformly to offer a continuous contact surface with the commutator segments was not necessary. Instead, a metal graphite brush was selected. These brushes contain graphite and a metal power, often electrolytic copper. [13] The metal powered helps lower the resistance of the brushes but causes them have a low elasticity which can cause the brush to fail at greater system RPM. The compulsator is within the recommended angular velocity of the brushes. The graphite-copper brushes will have a resistance on the order of 1 $\mu\Omega$.

This is also on the order of the commutator. This amount of resistance can be ignored in the compulsator system and in fact must be ignored in the commutator as replacements were unable to be found. Replacements will not be found because the current commutator was donated to the project by an engineer working with the company called for a quote. If another commutator were chosen, more funding would have to be procured and the choice made by the compulsator team would not have the benefit of years of experience.

Commutator:

Even though measuring the resistance of the commutator turned out to be unnecessary, when taking the measurement previously unseen damage was found. When the commutator was received it was found that the inner diameter that fits onto the shafting was not measured or possibly reported correctly, thus the commutator could not be fixed to the rotor. The mechanical engineers bored out the center enough to allow it to be attached but in doing so did damage to the commutator segments. The clamp or jig that was used to secure the commutator depressed into the soft copper segments. When the resistance measurement was taken it was expected that there would be some small variations in the resistance of each segment but it was found that they all measuring the same. Conductivity tests were performed between all the segments and it was found that the copper had been deformed in such a way as to cause a short throughout the commutator. If this had not be observed before the first spin up of the machine, even the lowest of RPM tests could have irreparably damaged the commutator. A dremel tool with small cone sanding attachment was used along the grooves in between the segments to ensure that there were not more shorts and the work was verified with further conductivity tests between all of the segments.

Skin Effect:

During the initial design phase a mistake was made while calculating the frequency of the system that caused an error of two orders of magnitude. The mistake arose from the lack of cross checking of work across the disciplines in this interdisciplinary team. When work is checked by the group as a whole, even if the knowledge is outside of the course work taken by some, simple data entry errors such as the one that caused the large frequency discussion can be avoided easily. It is important for any interdisciplinary team to take the time to explain their work despite the different knowledge levels.

The equation for the frequency of the compulsator is give below.

$$f = \frac{n * P}{120}$$

n is the velocity of the rotor in rpm and P is the number of poles. With a maximum velocity of 5000 rpm and a four pole machine the electrical frequency is 83.3 Hz. Initially the frequency was calculated to be ~35 KHz. While this is incorrect, the resulting tests on the effects of high frequency AC signals on our windings will still be useful in future air core compulsator systems that can reach frequencies of this magnitude.

The skin effect occurs when conductors are subjugated to high frequency signals. The skin effect limits the amount of the conductor's actual area used by limiting the current carrying part of the conductor to the surface. Conductors that have a radius larger than the skin are simply wasting space and materials because the center of the conductor will not carry any charge. The skin effect depth is approximated by the following equation. [7]

$$\delta = 503 \sqrt{\frac{\rho}{f * \mu}}$$

δ is the skin depth in meters, ρ is the resistivity of the material, f is the frequency of the system, and μ is the magnetic permeability of the material. The skin depth for our conductors is 3.6e-3 m. This means that anything larger than 7 AWG wire would contain wasted material. While a larger gauge wire does have less resistance per length than the smaller gauge, the increased difficulty in working with the material and the extra turns that can be fit into the rotor with smaller conductors more than makes up for this.

The skin effect also increases the resistance of the conductor. Since a low resistance is critical to our system performance this must be explored in higher frequency systems. The AC resistance of the conductor given the skin effect is calculated in the equation below.

$$R_{ac} = \frac{l_{phase} * \rho}{D * \pi * \delta}$$

l_{phase} is the length of one phase of windings, ρ is the resistivity of the material, D is the diameter of the conductor, and δ is the skin effect depth in meters. For the initially assumed frequency of ~35 KHz the AC resistance from the skin effect is only 2e-12 Ω. This value is negligible when compared to the mili-ohm resistance seen in the rest of the system. If the

frequency increased above 100 KHz the very small diameter conductor with shallow skin effect depth could see non-negligible AC resistances.

       To assure that no further calculation errors had been made and to test to see if Litz wire would be required due to high resistance, three lengths of wire had their resistance measured with a 335 Hz and a 20 KHz signal present. Nominal resistance, measured without a signal present, was used as a control to compare the other measurements to.

PURPOSED TESTING

At the time of this writing, compulsator fabrication was still in progress. Rotor fabrication was nearing completion but it was known that scheduling necessary rotor balancing and systems safety checks by Cal Poly employees would extend testing beyond the due date for this paper. This has happened due to delays from parts orders, discovering the error made when designing with the permanent magnets and then having to redesign many parts of the system, and the difficulty in coordinating the work of seven students between three systems. The complusator components have all be purchased, the designs updated, and the fabrication and testing schedule has been extended as needed. An outline of the testing the will be performed is given below.

Initial tests of the compulsator will begin at 50 RPM and increase in steps of 25 RPM up to 500 RPM until the safety and balance of the system have been confirmed. These tests will be performed with the compulsator, prime mover, and testing equipment only to minimize the systems at risk. During this tests, visual inspection of the test bed for vibrations, temperature readings from BK Precision TP-29-ND thermocouple, and prime mover input will all be used to verify the proper operation of the compulsator. Visual inspections are used to see vibrations from improper balancing, loose components, and other readily available clues to major issues. Temperature readings will confirm that the machine is rotating properly as without discharging under low speeds there should be very little heating in the system. Calculations of the required control of the prime mover with compulsator can be confirmed with RPM measurements taken from a WarpSpeed electric vehicle tachometer. [14] If the calculations are not correct and the prime mover requires a larger power input to turn the compulsator then there could be problems with physical components such as the bearing and must be explored before full RPM tests can proceed. The tachometer has been purchased but has not been adapted to fit the compulsators shafting but the prime mover has still not arrived. The prime mover has not been ordered but the calculations for the required input power to rotate are found in text books and only require the name plate information.

Once the safety of the machine is confirmed at 500 RPM, the steps in RPM will increase to 100 and the compulsator will be connected to the ignitron switching circuitry. Again for safety reasons the EMRG will not be connected. The ignitrons will discharge into a copper bar with the same resistance as the EMRG. These tests will continue until the compulsator reaches half power at 2500 RPM. Measurements of voltage, current waveforms for both phases, current into the

interpoles, and the measurements from the previous tests will be taken during each step. The current wave forms will be captured by Rogowski coils. These coils will be used because they do not have an iron core that can saturate, thus they respond nearly linearly to large currents.

Special attention to the temperature of the system and the state of the commutator during each discharge must be paid. The commutator and brushes should be examined for physical damage such as chipping or cracking of the brushes or commutator segments and discoloration or burns on the brush wires or commutator segments. See Figure 17 below for images of these kinds of damage. The rotor winding connections to the commutator should be checked several times as well though fewer problems are foreseen with these.
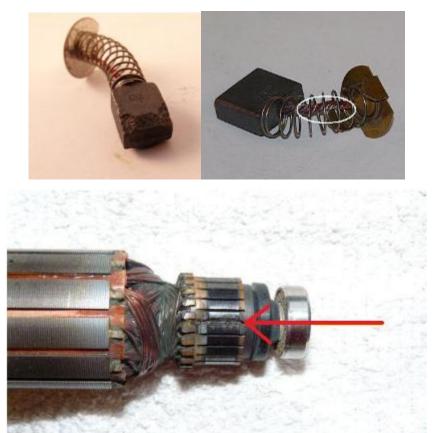
Figure 17: Images of brush and commutator segment damage[15]

The final stage of testing will increase the RPM from 2500 to 5000 in steps of 500 RPM. The compulsator will be discharged into the EMRG during these tests. If a control scheme for

the firing of the compulsator and automation of data collection through lab view has been finished it should be tested during this stage. Previous tests did not offer significant strains on the system so it was okay to leave all of these steps to manual activation. As the compulsator reaches the limits of its design the stresses on the systems should be minimized by creating an automated control scheme that will discharge the system the moment it is ready to fire. This control is also needed for data acquisition as measurements over the entire charge and discharge cycles. This will allow for the exploration of every stage of the EMRG firing process while delineating the results and removing human timing errors. The analysis of this data will focus on characterizing the compulsators output and comparing it to system modeling.

OPPERTUNITIES FOR FUTHER DEVELOPMENT AND STUDY

Once the compulsator has been fabricated and its safe operation has been achieved there are many aspects of its performance that could be modeled for the subject of senior projects. Most importantly a model of the machines internal inductance and its effect on efficiency would be very beneficial to future compulsator designs. Mechanical modeling and analysis would also be useful to future compulsator builds, especially analysis and design that would allow for greater tip speeds in future machines. Greater funding for future pulsed power projects has been given to the club founded by this team, Cal Poly Pulsed Power. With this reduction in budget constraints, an air cored compulsator design and fabrication could be explored.

Magnetic analysis of the permanent magnet rails and of the compulsator as a whole could constitute senior projects by themselves. Approximations were calculated for the strength of the interpoles and the effect of armature reaction on the permanent magnet field was ignored. Both of these could be verified and explored for a more exact model of the system.

Other aspects of this project besides the modeling of the compulsator could be expanded upon as well. The data acquisition system will need to be designed and purchased when funds are available. There are physics modeling of the system that could be explored, especially where the behavior of the projectile in the barrel and the behavior of the plasma generated during discharge were concerned.

Pulsed power systems have many applications outside of power supplies for EMRGs such as electroplating and fusing materials, pulsed lasers, pulsed water and waste treatment plants, and even for the pasteurization of food products. Teams for these projects would include the same engineering disciplines as the current project along with business, biomedical, and even agriculture. All of these systems will also need supporting facilities such as vacuum chambers or pasteurization tanks that will need to be designed and built along with the pulsed power supplies.

BIBLIGORAPHY

Web References:

1.   http://www.rare-earth-magnets.com/p-27-nsn0607.aspx

2.   http://ares.jsc.nasa.gov/education/websites/craters/lgg.htm

3.   http://image.ec21.com/image/tfautoparts/OF0010327161_1/Sell_Dc_Machine_Commutator.jpg

4.   http://people.msoe.edu/~saadat/download/lap_winding.pdf

5.   http://www.digikey.com

6.   http://www.ibsmagnet.com/knowledge/flussdichte.php

7.   http://en.wikipedia.org/wiki/Skin_effect#Formula

8.   http://en.wikipedia.org/wiki/Force_between_magnets#Force_between_two_bar_magnets

9.   http://ww2.momentive.com/Products/TechnicalDataSheet.aspx?id=3994

10.   Putley, D., R. C. McLachlan, and D. A. Hughes. "Design Conciderations For Compulsator Driven
        Railguns." *Ieee.org*. 6 Aug. 2002. Web. 29 Apr. 2012.
        <http://ieeexplore.ieee.org.ezproxy.lib.calpoly.edu/stamp/stamp.jsp?tp=&arnumber=22584>.

11.   http://www.kjmagnetics.com/calculator.repel.asp?calcType=block#

12.   http://www.allaboutcircuits.com/vol_1/chpt_8/9.html

13.   http://www.engineeringcarbonproducts.com/types_of_carbon.php

14.   http://www.rechargecar.com/product/warptm-speed-sensor

15.   http://www.ereplacementparts.com/article/968/Diagnosing_Electric_Power_Tools_101.html

Other Reference:

16.   PS-2162 2-Axis Magnetic Field Sensor datasheet, PASPort

17.   Fitzgerald, A. E., Charles Kingsley, and Stephen D. Umans. *Electric Machinery*. Fifth ed. New
        York: McGraw-Hill, 1990. Print.

18.   Chapman, Stephen J. *Electric Machinery Fundamentals*. Fourth ed. New York: McGraw-Hill,
        2005. Print.

19.   Rajput, R. K. *Electrical Machines*. Bangalore: Laxmi Publications, 2007. Print.

Category	Amount	Cost Per	Estimated Cost	S&H Cost (most estimated)	Taxes (calculated)	Source / Vendor	Supplier/Contact Info	More Info
Stator Material								
Aluminum Stator Casing	1 ft	$189.00	$189.00	$56.70	$14.65	MetalsDepot	MetalsDepot.com	P/N T310
1.25T Magnets	40	$13.87	$554.80	$17.06	$43.00	MagCraft	rare-earth-magnets.com	P/N NSN0607 (packs of 4)
Aluminum bar (1"x1") for interpoles and magnet rails	2	$36.18	$72.36	$21.71	$5.61	MetalsDepot	MetalsDepot.com	P/N SQ31 (2x6ft bars)
Flanges for stator (1/4"x2")	1	$17.82	$17.82	$5.35	$1.38	MetalsDepot	MetalsDepot.com	P/N F4142 (6 ft)
Stator Mounting Nuts	1	$4.44	$4.44	$1.33	$0.34	McMaster	McMaster.com	P/N 9713A250 (Packs of 10)
Stator Mounting Bolts	1	$11.13	$11.13	$3.34	$0.86	McMaster	McMaster.com	P/N 91247A732 (pack of 10)
Interpole/Mag. Rail Bolts	5	$6.99	$34.95	$10.49	$2.71	McMaster	McMaster.com	P/N 92240A750 (packs of 10)
Rotor Components								
Copper Wire 10 AWG (in ft)	347.5	$0.40	$139.00	$41.70	$10.77	Magnets4less	Magnet4less.com	
Aluminum Plate (t=1/16") 12"x12"	1	$19.09	$19.09	$5.73	$1.48	Speedy Metals	speedymetals.com	
Steel Flywheel (8in OD) 10in length	1	$351.90	$351.90	$105.57	$27.27	Speedy Metals	speedymetals.com	1018 Hot Rolled
Brake side Angular contact Roller Bearing (Bore 1.181)	1	$272.75	$272.75	$81.83	$21.14	McMaster	McMaster.com	P/N 2385K46
Clutch side Angular contact Roller Bearing (Bore 0.78")	1	$224.16	$224.16	$67.25	$17.37	McMaster	McMaster.com	P/N 2385K44
Flanges for rotor	1	$14.08	$14.08	$4.22	$1.09	MetalsDepot	MetalsDepot.com	P/N P114 (1"x1"-1/4" thick)
Brushes and Brush Holders	8	$20.00	$160.00	$48.00	$12.40	Waiting For Quote		
Commutator (Kirkwood 16 Bar)	1	$0.00	$0.00	$0.00	$0.00	Kirkwood	Donated from Kirkwood	0.7855" bore
Prime Mover Components								
16 Tooth Pinion	1	$19.14	$19.14	$5.74	$1.48	McMaster	McMaster.com	P/N 5172T21
48 Tooth Gear	1	$47.00	$47.00	$14.10	$3.64	McMaster	McMaster.com	P/N 5172T24
Studs (6" long 3/8"-16)	4	$2.00	$8.00	$2.40	$0.62	McMaster	McMaster.com	P/N 98750A080
Nuts (3/8"-16)	4	$0.00	$0.00	$0.00	$0.00	HomeDepot		
0.625" bearing for pinion shaft	1	$14.88	$14.88	$4.46	$1.15	McMaster	McMaster.com	P/N 2780T22
Friction Brake	1	$327.61	$327.61	$98.28	$25.39	Nexen Group	Applied Tech/805-928-1864::Quote-13964	P/N 841600, 842100 & 8420...
Magnetic Clutch	1	$294.79	$294.79	$88.44	$22.85	SDP-SI	SDP-SI.com	P/N S90C3C-30A1010
Pinion Shafting (5/8" OD) 2ft Length	1	$5.92	$5.92	$1.78	$0.46	MetalsDepot	MetalsDepot.com	P/N R258
Gear Shafting (7/8" OD) 2ft length	1	$13.58	$13.58	$4.07	$1.05	MetalsDepot	MetalsDepot.com	P/N R278
brake Shafting (1.25" OD) 1ft length	1	$11.46	$11.46	$3.44	$0.89	MetalsDepot	MetalsDepot.com	P/N R2114
Pinion Shaft Bearing (Bore .625")	1	$21.65	$21.65	$6.50	$1.68	McMaster	McMaster.com	P/N 8258K21
Single Phase Induction Motor	1	$380.00	$380.00	$114.00	$29.45	McMaster	McMaster.com	P/N 5990K23
Base Components								
Steel Mounting Bars for Stator (1 1/2"x3")	1	$130.16	$130.16	$39.05	$10.09	MetalsDepot	MetalsDepot.com	P/N F223 (4ft)
Endplate Bolts to Mounting Bars for Stator	2	$10.78	$21.56	$6.47	$1.67	McMaster	McMaster.com	P/N 90201A429 (Packs of 5)
Endplates (1ftx2ftx1in)	2	$167.02	$334.04	$100.21	$25.89	MetalsDepot	MetalsDepot.com	P/N P11 (1ftx2ftx1in)
5/16-18 Brake Fastener	1	$8.13	$8.13	$2.44	$0.63	McMaster	McMaster.com	P/N 91309A583
Subtotal Estimated Cost	$3,703.40							
Subtotal Taxes	$287.01							
Subtotal Shipping	$961.64							
Total	$4,952.05							

This table shows the part lists and costs for the compulsator.

APPENDIX B: EMRG TOTAL FUNDING AND PROJECTED COSTS

Project	Budgeted Cost	Projected Expenditures	Current Expenditures	Projected Remaining Funds	Actual Remaining Funds
Compulsator Project	$ 5,500.00	$ 4,956.97	$ 4,956.97	$543.03	$543.03
Test and Analysis of EMRG Mk. 1	$ 1,000.00	$ 695.03	$ 695.03	$304.97	$304.97
Barrel design attempts	$ 1,000.00	$ -	$ -	$1,000.00	$1,000.00
Projectile Manufacturing	$ 200.00	$ 81.80	$ 81.80	$118.20	$118.20
Safety	$ 500.00	$ 5.00	$ 5.00	$495.00	$495.00
DAQ System	$ 200.00	$ 6,082.54	$ 128.14	-$5,882.54	$71.86
Cap Bank Mk. 2	$ 2,000.00	$ 201.00	$ 201.00	$1,799.00	$1,799.00
Mfg and Test of EMRG Mk. 2	$ 1,300.00	$ -	$ -	$1,300.00	$1,300.00
Vacuum Chamber	$ 2,000.00	$ -	$ -	$2,000.00	$2,000.00
Totals:	$ 13,700.00	$ 12,022.34	$ 6,067.94	$1,677.66	$7,632.06

The above table shows the projected costs of the first EMRG system able to reach testing velocities. This has been included to show the scale of cost for the compulsator with the rest of the system and how must money would be needed to meet the system requirements.

APPENDIX B: MAGNETIC ANALYSIS MODELS